Estuaries Vol. 23, No. 3, p. 367–380 June 2000

Net Circulation and Salinity Variations in an Open-Ended Swedish Fjord System

GÖRAN BJÖRK[1]
OLOF LIUNGMAN
LARS RYDBERG
Göteborg University
Earth Sciences Centre/Oceanography
Box 460, SE-405 30 Göteborg, Sweden

ABSTRACT: Water circulation and salinity variations above sill levels in the Orust Tjörn fjords on the Swedish west coast, are investigated by means of hydrographic observations and a process-oriented box model. This fjord system, which is situated in the outer part of the Baltic estuary, consists of several basins separated by a number of sills and narrow passages. In contrast to most fjords, it is connected to the sea at both ends. Current measurements at different locations indicate a net, counterclockwise (mainly northward) circulation with an average of about 100 $m^3 s^{-1}$. Model results and analyses of observations show that this net subtidal through-flow is primarily forced by the difference in steric height between the open ends. Salinity variations in the coastal waters give rise to density driven currents, mainly from the south which dominate the fjord exchange at large. The subtidal net circulation may be important for the properties in the northern parts of the system, particularly during periods of reversal. Validation against measurements shows that the model captures variations in the net circulation, as well as variations of the basin salinities above sill level. A seven-year model run, using monthly hydrographic data as forcing, yielded that the net circulation was counterclockwise during 81% of the time with a long-term average flow of about 70 $m^3 s^{-1}$. Tidal choking in the narrow, northern end increases the flow resistance substantially, thereby decreasing the net through-flow.

Introduction

The steric height, or its equivalent in pressure space, the dynamic depth (e.g., Tomczak and Godfrey 1994), has long been used to estimate sea level variations and ocean circulation from hydrographic data. By adopting a level of no motion it is possible to calculate geostrophic velocities in the surface waters of the open ocean (e.g., Eid and Said 1995; Ridgway and Godfrey 1997). In coastal waters, particularly in estuaries with large salinity gradients, the steric height may dominate the sea level variations on time scales longer than a few days. Patullo et al. (1955) showed a seasonal sea level range of 41 cm in the inner Bay of Bengal due to variations in the freshwater input. Lizitzin (e.g., Lizitzin 1974) and recently Carlsson (1998) studied seasonal and longitudinal variations in the mean sea level topography of the Baltic Sea. They showed that the steric height is the single most important effect determining these variations, which have a magnitude of 10–20 cm. Within this context, the present paper offers an example of how the difference in steric height between two locations in the outer part of the Baltic Sea estuary, near the Swedish west coast, can be used to model long-term variations in the net circulation through a series of connected fjords.

The fjord system inside the islands Orust and Tjörn on the Swedish west coast consists of several fjord basins with intermediate sills and narrows. Maps of the fjord area and its surroundings are shown in Figs. 1 and 2. The hydrography of the fjord system is strongly influenced by low saline Baltic water, which affects the surface waters of Kattegat and Skagerrak (Fig. 1). This imposes a salinity stratification within the entire fjord system, whereas local freshwater supply is of minor importance.

Because the fjord system is sheltered and the tides are weak, anoxic conditions are common in the deep inner basins below the halocline. Coastal eutrophication may have worsened the situation (Nilsson and Rosenberg 1997). The surface water nutrient levels are 50% higher than those of the coastal waters, a difference which is not readily explained as an entirely local effect (Axelsson and Rydberg 1993). High chlorophyll and POC values indicate that the primary production is enhanced compared to that of Kattegat and Skagerrak. Another odd feature is the lack of diarrhetic shellfish poison (DSP) in mussels from the inner parts of the fjord system, particularly Koljöfjorden. Haamer (1995) suggested that high silicate concentrations in the system are unfavorable for the development

[1] Corresponding author; e-mail: gobj@oce.gu.se.

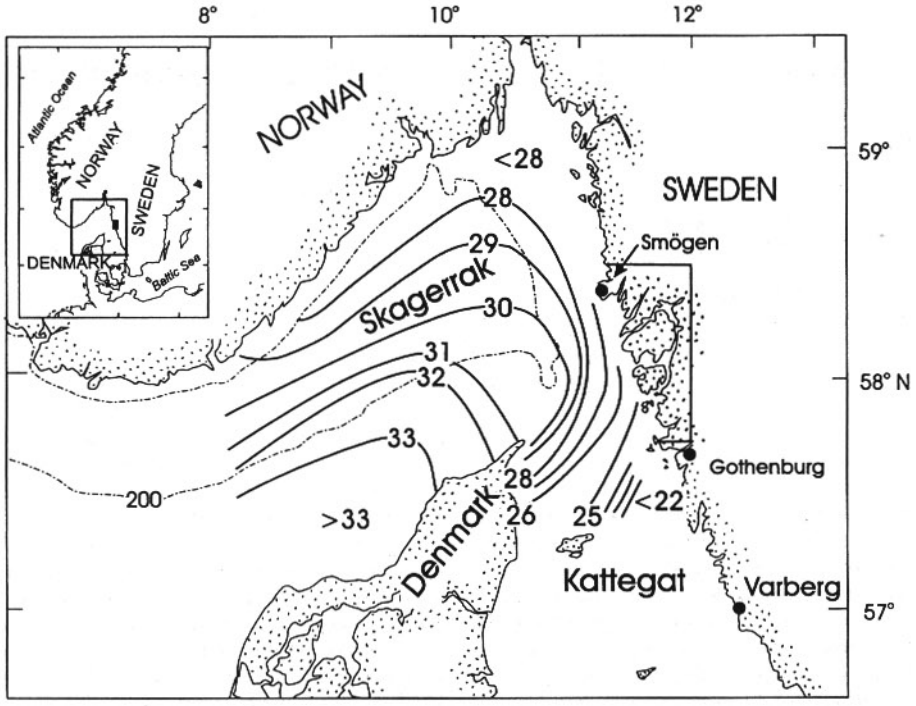

Fig. 1. Map showing the location of the Orust Tjörn fjord system on the west coast of Sweden. Also shown is the average field of surface salinities in Skagerrak and northern Kattegat May–August (from Rodhe 1996).

of toxic algae forms and that the exchange processes are too slow to bring in such algae from the Skagerrak, where DSP is a recurring problem.

Since 1990, local authorities on the Swedish west coast have operated a comprehensive monitoring program (BOSAM) with several stations located within the fjord system and along the coast. Axelsson and Rydberg (1993) noted that the BOSAM program offers a very good insight into the hydrography and nutrient conditions, but that it suffers from lack of reliable estimates of water exchange, suggesting complementary current and sea level measurements. We commenced such a program in 1994 with the ultimate aim of presenting a biogeochemical model for the entire fjord system.

Successful models for generating water exchange in fjords caused by variable external stratification were recently developed by Stigebrandt (1990), Engqvist and Omstedt (1992), and Gillibrand et al. (1995). The Orust-Tjörn fjord system differs from most fjords in that there are openings at both ends, a feature which allows for a net through-flow of water. This paper presents a process-oriented model of the circulation in the fjord system, which combines baroclinic exchange due to variations in the external salinity stratification with a (sub-tidal) through-flow driven by the difference in steric height between the northern and southern entrances. The model is forced by monthly hydrographic data from the BOSAM program. The verification is based on a combination of BOSAM data, for comparing the salinities, and our data for comparing current velocities and through-flow.

Study Area

Topography

The fjord system consists of four main basins (Fig. 2). Beginning from the south they are: Hakefjorden, Havstensfjorden, Byfjorden, and Koljöfjorden. The basins are connected to each other by shallow and narrow constrictions such that there are individual sill basins in Havstensfjorden, Byfjorden, and Koljöfjorden. At the northern end there are two narrow channel systems, Malö Strömmar and Nordströmmarna, connecting Koljöfjorden to Skagerrak. Malö Strömmar, the deeper of the two, includes two channels, Björnsund and Malösund, which have both been blasted to a depth of 9 m, a minimum width of approximately 40 m, and a length of about 250 m. The sill depth in Nordströmmarna is less than 5 m. The southern entrance, between Hakefjorden and Skagerrak, is deep and wide, with an approximate sill depth of 25 m and a width of several km. There is also a third, but more narrow connection to the sea

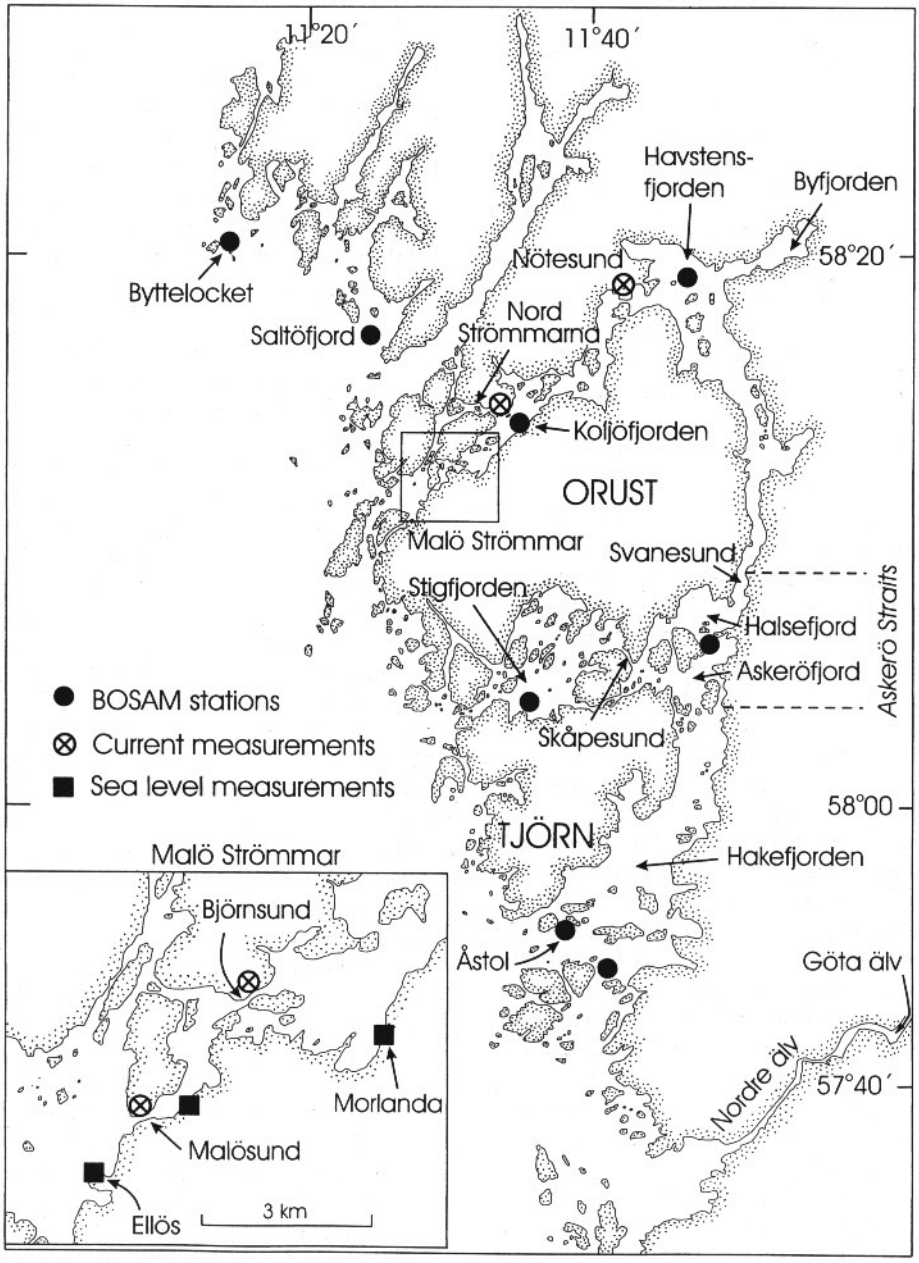

Fig. 2. Map of the fjord system showing positions for the stations within the BOSAM program including sites for current and sea level observations during the campaigns in 1994–1996.

through Skåpesund and Stigfjorden, between the islands Orust and Tjörn. The constriction between Havstensfjorden and Hakefjorden has its most narrow and shallow cross section at Svanesund with a sill depth of 20 m, but there are also a series of small sub-basins just south of Svanesund, Askerö-fjorden, and Halsefjorden, connected by slightly wider constrictions. In what follows we will use the term Askerö Straits for this series of constrictions. The sill depth in Nötesund, between Havstensfjorden and Koljöfjorden, is 10 m. Byfjorden is connected to Havstensfjorden through Sunningen with a dredged sill depth of 12 m. The main topographic features of the fjord system are summarized in Table 1.

Hydrography and Circulation

The surface water salinities in the eastern Skagerrak are highly variable, being dominated by the changing outflow from the Baltic (Anderson and

TABLE 1. Some topographical characteristics of the fjord system.

Model Notation	Value	Unit	Topographic Feature
	5,000	m^2	Cross section Askerö Straits
	2,300	m^2	Cross section Nötesund
A_M	325	m^2	Cross section Björnsund
A_{Nord}	230	m^2	Cross section Nordströmmarna
H_A	20	m	Sill depth Askerö Straits
H_N	10	m	Sill depth Nötesund
H_M	9	m	Sill depth Malö Strömmar
b_A	250	m	Equivalent width Askerö Straits
b_N	230	m	Equivalent width Nötesund
b_M	36	m	Equivalent width Malö Strömmar
	61 ± 10^6	m^2	Surface area Havstensfjorden
	29 ± 10^6	m^2	Surface area Koljöfjorden
	6 ± 10^6	m^2	Surface area Byfjorden

Rydberg 1988). In the area outside the fjord system, Kattegat surface water with salinities (S) in the range 20–30 and a depth of 5–20 m, meets high saline Skagerrak water, which circulates counterclockwise around Skagerrak (S = 32–35; Rydberg et al. 1996). The high frequency variability of the surface layers in the frontal area is described by Gustafsson (1999). It is shown that the frontal structure is strongly coupled to the wind direction, such that winds with a westerly component tend to sharpen the front and force it southwards, while easterly winds spread the Kattegat surface layer and produce a front more parallel to the Swedish coast. The frontal structure responds on the order of days to shifting wind direction. The variance field of the surface density in Skagerrak and in northern Kattegat has a maximum, indicating the mean location of the front, just outside the southern end of the fjord system (Gustafsson and Stigebrandt 1996).

Within the fjord area, the sills and narrows exert a profound impact on the hydrography by stabilizing a characteristic two-layer stratification with halocline depths of 10–15 m. The variations in the halocline depth is less pronounced than in the coastal waters outside, whereas the salinities are similar; the surface water salinities are found in the range 22–25 (0–10 m) whereas the deep water salinities are about 28–32 (20 m), with the lowest values in Koljöfjorden (Axelsson and Rydberg 1993). Tides are weak, with a spring tidal range of about 30 cm.

Although the literature on water circulation within the fjord system is sparse, there are at least two independent observations of a net subtidal counterclockwise through-flow in the fjord system. In both cases, the measurements are from Nötesund. Ehlin (1971) observed a mean westward current of about 4.5 cm s^{-1} during a 3-mo period in 1967. In 1974, an Aanderaa current meter deployed for 1.5 mo also indicated a westward mean velocity of 5–10 cm s^{-1} (Cederlöf and Djurfeldt personal communication). The velocities correspond to a transport of the order of 100 m^3 s^{-1}. Unpublished data from current measurements, referred to by Ehlin (1971) and by Cederlöf and Djurfeldt (personal communication), also indicate strong baroclinic flows in the Askerö Straits and further south in the fjord system.

Observations and Data Treatment

Field Program 1994–1996

Our field program during 1994–1996 was directed towards studies of water circulation and through-flow and consisted of sea level and current measurements at several sites within the fjord area. Current measurements at the Nötesund sill, in the central fjord area (Fig. 2), were carried out between October 20 and November 29, 1994 using a bottom mounted Acoustic Doppler Current Profiler (ADCP) from RD Instruments. Tide gauges (MicroTide) were deployed at the northern end of the fjord system, on both sides of Malö Strömmar (at Ellös and Morlanda), from October 17 to November 29, 1994, from November 9 to December 27, 1995, and from March 31 to June 4, 1996. In order to level the tide gauges and to tune a model for calculating the volume flux from the sea level difference along Malö Strömmar, current measurements with RCMs (Sensordata SD-6000) were undertaken in Björnsund (Fig. 2) during shorter periods. The current meters were positioned at different positions and depths, to make sure that there were no baroclinic effects in this area, as well as to determine the volume flux. A salinity-temperature chain (Aanderaa) with four sensors, positioned at depths from 3 to 20 m, was deployed near Åstol, in the southern end of the fjord system, from March 13 to May 31, 1996. The measurements from 1994 and 1995 were published in Liungman et al. (1996).

To determine the volume flux through Malö Strömmar, the instantaneous current speed u'_M in Björnsund was computed from the sea level difference η_M between Ellös and Morlanda (Fig. 2) using a modified Bernoulli expression (Stigebrandt 1980),

$$u'_M = \sqrt{\frac{2g}{C_M}\eta_M} \tag{1}$$

where C_M is a constant greater than 1, that depends on the frictional resistance in the straits (see Appendix). This formula, as indicated by a 2-wk comparison from 1995 shown in Fig. 3, accurately describes the barotropically forced flow in the channel. The value of C_M was determined from periods

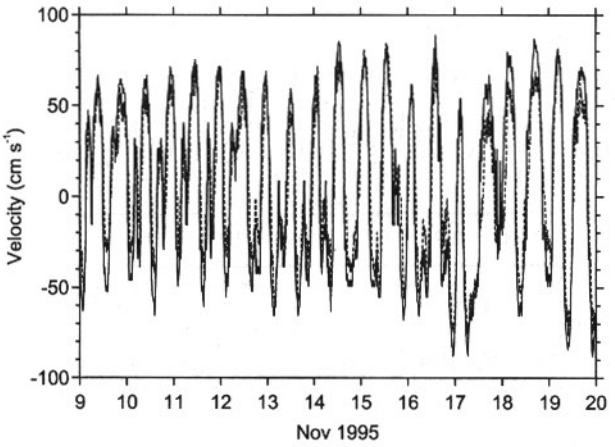

Fig. 3. Current speed in Björnsund during 12 days in 1995. The dashed line shows the velocities from a recording current meter at 1.5 m above the bottom. The solid line is computed from the sea level difference between Ellös and Morlanda (for positions see Fig. 2).

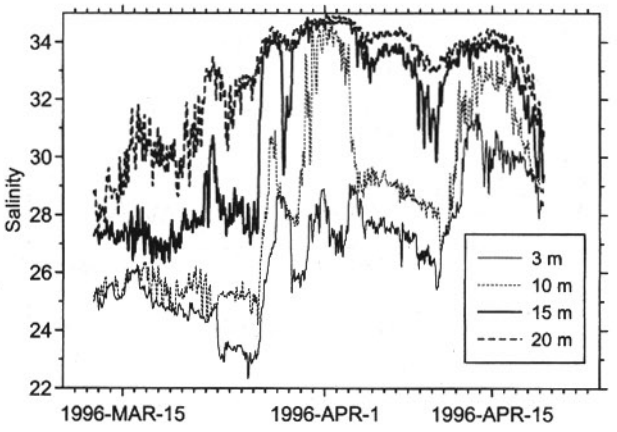

Fig. 4. Time series of salinity at four depths, from a T-S chain deployed close to Åstol in March–April 1996.

of simultaneous current measurements in Björnsund and sea level observations at Ellös and Morlanda. The tide gauges were leveled using instances of zero current velocities, assuming that the sea level difference should also be zero. C_M was then calculated through a least-squares fit between the measured sea level differences and the square of the current velocities at all times. We estimated the constant C_{Nord} for Nordströmmarna, using current measurements from the southern end of this, more narrow channel system and the same sea level observations as above. The values of C_M and C_{Nord} were found to be 2.7 and 5.5, respectively.

Figure 4 shows time series of salinities from the salinity-temperature chain deployed near Åstol. It indicates strong fluctuations on time scales which are much shorter than 1 mo. During most of the time there is a two-layered structure, although the salinities vary substantially. Short-term fluctuations will impose an uncertainty in the forthcoming analysis, which by necessity is restricted to the monthly BOSAM observations.

Although the tidal range along the Skagerrak coast is small, a sea level record from one of our stations in the fjord area (Fig. 5) clearly indicates the dominance of the semidiurnal tide. The sea level variations are otherwise affected by regional wind conditions and, to a lesser extent, by atmospheric pressure variations (Stigebrandt 1984).

The current measurements from Nötesund, using the bottom-mounted ADCP, are shown in Fig. 6a. These measurements indicate a mean westward velocity of 7.5 cm s^{-1} (Liungman et al. 1996), thus corroborating the existence of a prevailing counterclockwise circulation. Figure 6b,c shows the computed velocities in Björnsund from two periods during 1995 and 1996. Different from the measurements in Nötesund, these measurements do not indicate any prevailing net through-flow, but instead relatively long periods with flow in either direction. A common feature in all these series is a variability on time scales of 2–3 d superimposed on variations on longer time scales (10–20 d). In Nötesund there is also a very clear baroclinic signal, indicated by substantial differences in current velocities between the surface and the bottom, as measured by the ADCP (Fig. 6d). Some instances may also be discerned when the currents are in opposite directions. However, we did not see any vertical variations in Björnsund.

BOSAM Data

The BOSAM data for 1990–1996 were obtained from the Swedish Meteorological and Hydrological Institute (SMHI). This data set contains monthly observations of salinities at several depths (0, 2, 5, 10, 15, 20, and 25 m) from 7–8 stations within the

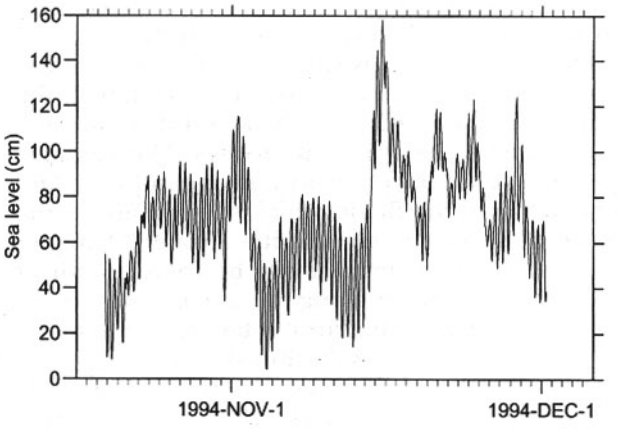

Fig. 5. A 1-mo sea level record from Morlanda inside the northern end of the fjord system (arbitrary reference level).

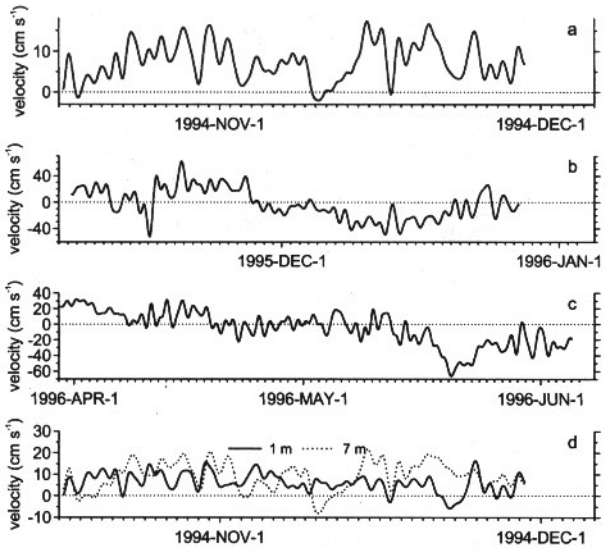

Fig. 6. Low-pass filtered currents at Nötesund and Björnsund, using a cut-off period of 26 hours. Westward, i.e., counterclockwise current is positive. (a) Vertically averaged ADCP velocities in Nötesund during November–December 1994. (b) Velocities in Björnsund during November–December 1995, computed from the sea level difference along the strait (see Eq. 1). (c) Velocities in Björnsund during March–May 1996, again computed from the sea level difference. (d) Velocities in Nötesund at 1 and 7 m, respectively during November–December 1994. The velocity data from Fig. 6a–c are those used in the comparison with the model computed net through-flow (see Fig. 13).

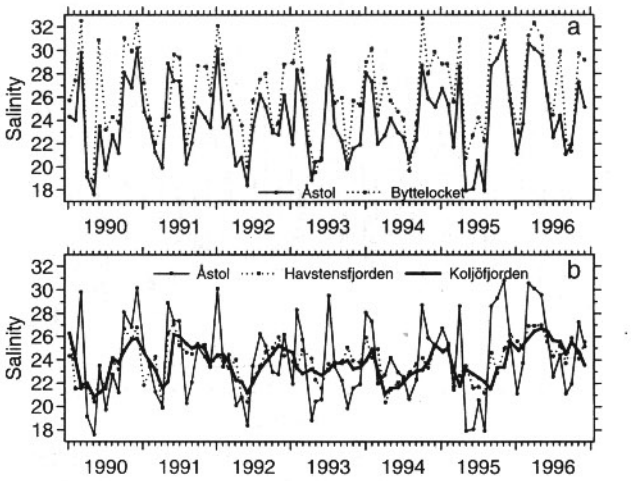

Fig. 7. Surface (0–10 m) salinity at selected BOSAM stations along the coast and within the fjord system. (a) Åstol and Byttelocket. (b) Åstol, Havstensfjorden, and Koljöfjorden. For locations see Fig. 2.

area, one in each fjord basin and a few in the coastal waters outside (Fig. 2). As a background for the process-oriented model, we will briefly discuss some features evident in the BOSAM measurements.

Figure 7a shows the 0–10 m mean salinity from two BOSAM stations outside the fjord system, Åstol and Byttelocket (Fig. 2). The salinity at the southern station, Åstol, varies between 18 and 30 and features strong fluctuations on time scales from 1 to about 6 mo. The salinity record at the northern station, Byttelocket, is similar to that at Åstol but the salinity is generally higher and occasionally the difference exceeds 5 units. Now and then, the gradient reaches zero or even reverses. This can happen as a result of consecutive strong inflow to and outflow from the Baltic, which strongly affects the Kattegat surface water salinities. Water of higher salinity may then temporarily be found south of more brackish water along the Swedish west coast. The waters within the fjord system clearly respond to the varying salinities within the upper layers of the Skagerrak and Kattegat. This is seen in Fig. 7b, where the salinity data from Havstensfjorden and Koljöfjorden are compared to those from Åstol. There is a correlation between the salinities inside the fjord system and those outside but there is also a gradual damping of the salinity variations with distance from the southern entrance. When comparing the salinity in Koljöfjorden with that at Byttelocket (Fig. 7a,b) there is, in addition to a large difference in amplitude, a generally lower salinity in Koljöfjorden. The mean salinity is 26.4 at Byttelocket, 23.7 in Koljöfjorden, and 24.0 at Åstol. A larger salinity difference between Koljöfjorden and Byttelocket than between Koljöfjorden and Åstol indicates that the water exchange through the northern straits is more restricted than through the southern straits. The local freshwater supply to the fjords is of minor importance but is probably the reason why the mean salinity in Koljöfjorden is somewhat lower than that at Åstol.

Exchange Mechanisms

Net Subtidal Through-flow

The sea surface slope along the coast is likely to be coupled to the so called steric effect, which tends to raise the sea level at places with a surface layer of low density, such that the horizontal baroclinic pressure differences are compensated for at depth. The steric effect has been shown to be of major importance in the Baltic estuary and should be pronounced across the Kattegat-Skagerrak front. Gustafsson and Stigebrandt (1996) estimated the seasonal variations of the steric height in the Skagerrak-Kattegat region from salinity observations and showed that the mean sea level is about 10 cm higher in northeastern Kattegat than in central Skagerrak. For the fjord case, we expect that the difference in steric height η_s between lo-

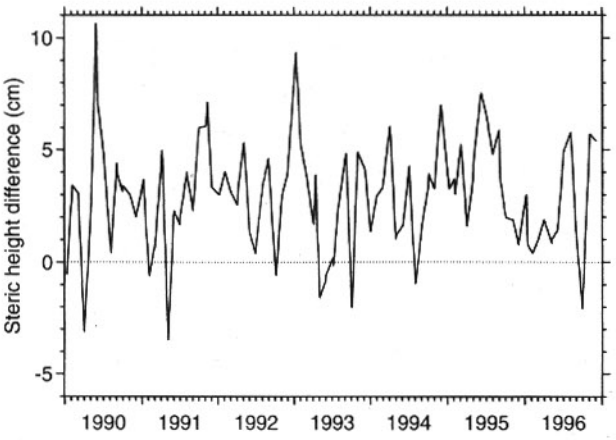

Fig. 8. The difference in steric height between Åstol and Byttelocket, η_S computed according to Eq. 2, from monthly salinity measurements within the BOSAM program.

cations just outside the two ends of the fjord system, can be estimated from the expression

$$\eta_S = \beta\left(\int_0^H S_B\, dz - \int_0^H S_A\, dz\right) \qquad (2)$$

where z is directed downwards with zero at the undisturbed sea surface and S_B and S_A are the salinities at the nearby BOSAM stations Byttelocket and Åstol. β relates the salinity to the density ρ according to $\partial\rho = \rho\beta\partial S$ (because of the large salinity differences we disregard temperature effects on the density). The depth of integration H is set to 20 m, since this is the greatest depth at which observations are always available at Byttelocket. This station was chosen to represent the conditions outside the northern end of the fjord system instead of the more closely located station at Saltöfjord (Fig. 2), since the record at Byttelocket is longer. The salinities at these two stations are practically identical. The time series of η_s for 1990–1996 (based on monthly observations) is shown in Fig. 8. Large variations are evident, with a maximum range of 13 cm. The overall average indicates a 2.8 cm higher sea level at Åstol.

Though 20 m may seem to be a rather shallow level of no motion, it should be emphasized that temporal and spatial salinity variations above the halocline greatly exceed those below. Since the halocline is usually found above 20 m, the steric height difference should be dominated by the conditions above 20 m. That this is actually the case is indicated by a calculation of η_s using H = 25 m, for those occasions when measurements at this depth are available at Byttelocket. Only for 2 instances out of 49 does the difference between calculating η_s for H = 20 and 25 m exceeds 2 cm. The standard deviation of the difference in η_s for the remaining 47 instances is only 0.58 cm.

Baroclinic Sill Flows

Another important process for the water exchange is the baroclinic flow associated with the adjustment of the water column inside the fjords to salinity variations in the coastal waters. The importance of this mechanism for the water exchange above the sill level in fjords has been shown in earlier investigations (e.g., Stigebrandt 1990). Figure 7b shows that the salinity variations outside the system propagate inward, indicating a large water exchange. It is also evident from the current observations in Nötesund (Fig. 6d) that baroclinic motions are common.

Other Forcing

The tidal currents generate water exchange between the different basins and between the fjords and the sea. Björk (1983) estimated a nominal exchange of the order of 1–2% of the volume above sill level per day. The efficiency of this exchange is mainly dependent on the tidal amplitude and the length of the strait compared to the tidal excursion length. In Malö Strömmar, the excursion length can be estimated from observed current velocities in Björnsund. The mean velocity at spring is 0.35–0.4 m s^{-1}. Because Björnsund is the narrowest part of Malö Strömmar (Fig. 2), a realistic estimate of the mean current velocity for the entire Malö Strömmar is 0.15 m s^{-1}. Since half a tidal period is about 6.2 h, the excursion length is approximately 3 km. As the length of Malö Strömmar is 3.4 km, we may conclude that the tidal exchange through Malö Strömmar, in the case of zero net flow, is small.

The ADCP measurements indicate that the vertically averaged mean tidal velocity in Nötesund is about 0.2 m s^{-1} at spring. This implies a corresponding tidal excursion length of about 4 km. The narrow part of Nötesund is very short, only a few hundred meters, which would imply an efficient tidal exchange through Nötesund. This is contradicted by the fact that salinity measurements in Nötesund show no correlation with current direction (Liungman et al. 1996) indicating that more or less the same water body is advected back and forth over the sill with the tide, thus implying a weak net exchange. Though perhaps not entirely justified, the conclusion is that tidal exchange can be neglected also in Nötesund.

The transport through Svanesund during one flood (or ebb) period should equal the sum of the tidal prism of the fjords north of Svanesund, minus the volume flux through Malö Strömmar and Nordströmmarna. Since the transport through

Nordströmmarna is roughly half of that through Malö Strömmar (Liungman et al. 1996), the flow through the northern end of the fjord system should equal 30×10^6 m^3, assuming a spring tidal range of 30 cm (Liungman et al. 1996). Using the cross-sectional area of Svanesund, the excursion length during spring is found to be almost 5 km, which is less than the length of Svanesund. We conclude that the tidal exchange through Svanesund is negligible.

The sea level record in Fig. 5 shows a few large, low-frequency variations, one of which reaches 1 m in range. Such large-scale wind driven sea level variations may in extreme cases induce important volume fluxes in the fjord system, although events such as that on November 15, 1994 are rare.

There is a local freshwater discharge averaging about 5 m^3 s^{-1}, mainly to Byfjorden and Havstensfjorden. Because the surface salinities in general show little or no decrease from Åstol to Havstensfjorden (Axelsson and Rydberg 1993), effects of locally driven estuarine circulation should be small enough to be neglected in the present context.

The local wind may affect the conditions in the fjords in different ways, but it is altogether unlikely that the local wind-forced surface current will have any significant effect on the net circulation or the water exchange. Comparing the ADCP measurements at Nötesund with the along-channel wind component shows almost no correlation at all. Only in the uppermost 1–2 m is there a weak tendency for the current to follow the wind. Wind mixing, on the other hand, affects the water exchange by changing the stratification and therefore the baroclinic fluxes. This effect is implicitly included in the model.

The Model

To test the hypothesis that the subtidal mean circulation is driven by the steric height difference along the coast and to quantify the baroclinic water exchange, we implemented a simplified, process-oriented box model. We believe that the possible importance of the steric height difference as a forcing mechanism is more clearly elucidated, and our understanding of the variations in the mean circulation better served, by using a process-oriented approach and a simple model. It would have been possible to digitize the topography and apply a fully 3-dimensional, primitive-equation model, but since the narrow constrictions towards the sea and between the sub-basins play a critical role in determining the circulation, a primitive-equation model would require high spatial, and hence temporal, resolution. It would not be a trivial task to set up such a model, and it is doubtful whether the results would be more enlightening considering the extra effort required, particularly in interpreting the vast amount of results and untangling the processes involved. The rather low temporal resolution of the boundary conditions clearly motivates a more simple, quasi-stationary box model.

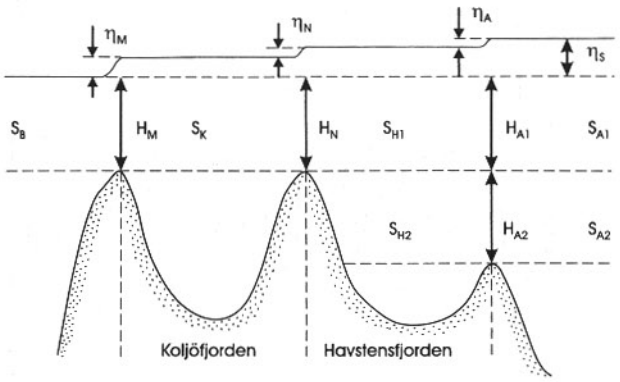

Fig. 9. Schematic sketch of the fjord model (see text for definitions).

The model consists of three fjord boxes, as shown in Fig. 9, one of which is for the entire surface water above the sill level in Koljöfjorden (0–10 m) and two (0–10 m, 10–20 m) for the water column above the sill level in Havstensfjorden. The geometry of the fjord system is further simplified such that the influence of Skåpesund (Fig. 2) is neglected and the sub-restrictions in Malö Strömmar and the Askerö Straits are not resolved. Byfjorden is treated as a passive reservoir adding to the volume of Havstensfjorden. The model is forced with the 0–10 m and 10–20 m mean salinity at Åstol and the 0–10 m mean salinity at Byttelocket. The velocity $u(z)$ through a strait is assumed to be controlled by the pressure difference at each depth according to the method used in Stigebrandt (1990). In the following we use indices A for Askerö Straits, N for Nötesund, and M for Malö Strömmar. Velocity at depth z in the Askerö Straits is given by

$$u_A(z) = \alpha_A \sqrt{2g(\eta_A + h_A(z))} \tag{3}$$

where g is the acceleration of gravity, α_A an empirical constant describing the baroclinic flow efficiency of the strait, η_A the sea level difference, and h_A the change in pressure height due to density differences across the Strait:

$$h_A(z) = \begin{cases} \beta(S_{A1} - S_{H1}) \\ \quad z \le H_{A1} \\ \beta((S_{A1} - S_{H1})H_{A1} + (S_{A2} - S_{H2})(z - H_{A1})) \\ \quad z > H_{A1} \end{cases} \tag{4}$$

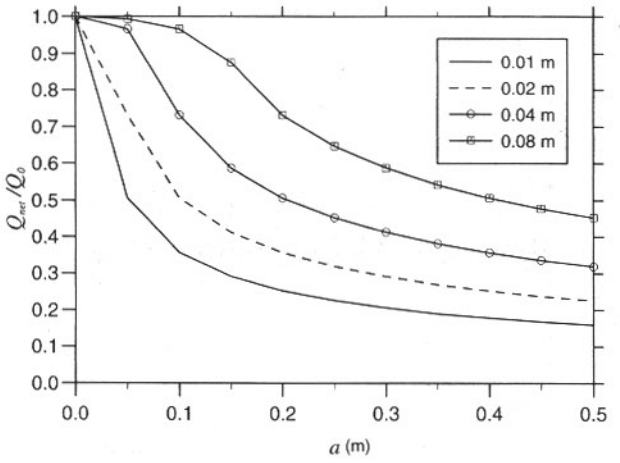

Fig. 10. Choking of the mean transport Q_{net}/Q_0 by tidal oscillation in Malö Strömmar as a function of tidal amplitude, a and for different values of the mean sea level difference over the strait. Q_0 is the mean transport in the case of no tidal oscillations ($a = 0$).

Here, $S_{A1,2}$ and $S_{H1,2}$ are the salinities in the upper/lower layer at Åstol and Havstensfjorden respectively, and H_{A1} is the thickness of the upper layer. The velocity in Nötesund is determined in a similar way as for the Askerö Straits with the simplification that there is only one layer on each side of the strait:

$$u_N(z) = \alpha_N\sqrt{2g(\eta_N + h_N(z))} \quad (5)$$

$$h_N(z) = \beta(S_{H1} - S_K)z \quad (6)$$

S_K is the salinity in Koljöfjorden. In Malö Strömmar and Nordsströmmarna, where the channels are shallow, long and narrow, the flow is primarily of a barotropic nature. This is also confirmed by current measurements (Liungman et al. 1996). The current may be determined from the sea level difference η_M alone, according to Eq. 1. In these straits, we may expect the tidal current to have a direct influence on the flow capacity because of tidal choking. To evaluate how the choking affects the mean flow, we constructed a simple model of Malö Strömmar and calculated the net transport for various combinations of mean sea level differences and tidal amplitudes. The model is described in the appendix and the choking effect is shown in Fig. 10. The sub-tidal velocity in Malö Strömmar is then defined as

$$u_M = k_M\sqrt{\frac{2g}{C_M}\eta_M} \quad (7)$$

where k_M is the tidal reduction factor. The flow through Nordströmmarna is described by a similar expression. Salinity differences across the Askerö Straits or Nötesund will result in depth dependent baroclinic flows described by the pressure difference terms Eqs. 4 and 6. In order to calculate the absolute velocity, the sea level difference η, separate for each constriction is also needed. This can be determined from volume continuity such that the total transport is equal for all three straits, i.e.,

$$Q_A = Q_N = Q_M \quad (8)$$

where

$$Q_A = b_A\int_0^{H_A} u_A\,dz \quad (9)$$

$$Q_N = b_N\int_0^{H_N} u_N\,dz \quad (10)$$

$$Q_M = k_M\left(\frac{A_M}{\sqrt{C_M}} + \frac{A_{Nord}}{\sqrt{C_{Nord}}}\right)\sqrt{2g\eta_M} \quad (11)$$

b_A and b_N are the widths of the straits, and H_A and H_N the total depths of the straits. A_M and A_{Nord} are the cross-sectional areas of Björnsund and Nordströmmarna, the latter at the location of the current measurements. The flow through Nordströmmarna has been added to the flow in Malö Strömmar using the notation Q_M for the combined flow in both straits. The second term in Eq. 11 is close to half the size of the first term, implying that about 30% of the total flow will pass through Nordströmmarna. The sea level difference across the entire fjord system, η_s is determined from the steric height difference between Åstol and Byttelocket (Eq. 2), while the sea level differences across the individual straits η_A, η_N, and η_M are calculated by an iterative procedure such that Eq. 8 is fulfilled together with the condition that the sum of the sea level drops over the individual straits should equal the steric height difference outside the system:

$$\eta_S = \eta_A + \eta_N + \eta_M \quad (12)$$

When η_A, η_N, and η_M are determined, a final computation using Eqs. 3, 5, and 7 yields the volume and salt fluxes through each strait. The basin salinities are then updated such that a layer of salinity equal to the salinity at the opposite side of the strait is supplied for each of the inflows to the basin. The resulting layers in each basin are sorted to ensure hydrostatic stability, and the time step ends with a procedure where the layers in each box are mixed to produce the new box salinity. Basin-wide mixing is implicitly assumed in the box discretization, though no specific process is proposed. Certainly, both wind and tidal mixing are important. As a result of the two-layer discretization, the sill flows can be either one, two or three-layered, but three layered only in the Askerö Straits where

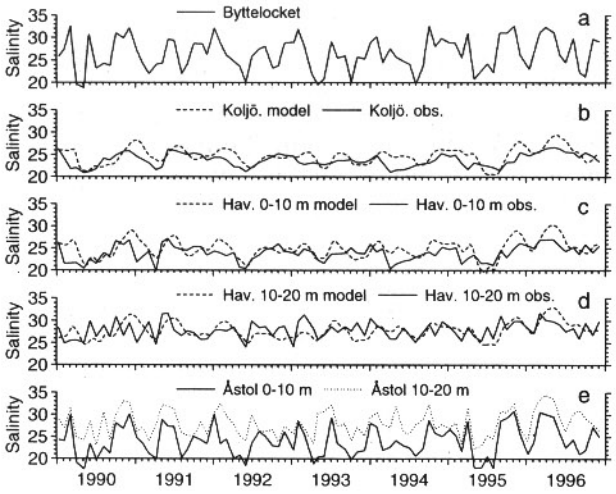

Fig. 11. Model-computed salinities compared to monthly observations obtained within the BOSAM program. (a) Observed salinity at Byttelocket. (b) Observed and computed salinity in Koljöfjorden. (c) Observed and computed salinity in Havstensfjorden 0–10 m. (d) Observed and computed salinity in Havstensfjorden 0–20 m. (e) Observed salinity at Åstol 0–10 m and 10–20 m.

a deep-water salinity difference may change the flow direction.

Model Results and Discussion

Volume Fluxes, Salinities and Sea Levels

The model was run for the period 1990–1996, using the monthly salinity profiles at Åstol and Byttelocket from which both the baroclinic and the barotropic forcing was derived. The three model coefficients k_M, α_N, and α_A, were determined to be 0.5, 0.25, and 0.15, respectively. The value for k_M was determined from Fig. 10 using a tidal amplitude of 20 cm and a mean sea level difference of 2 cm. We judged it an unnecessary complication in this rather rough model to use a k_M-value that varies with the mean sea level difference and tidal amplitude. We then reduced the coefficient α_A for the Askerö Straits in order to achieve an approximately correct amplitude for the salinity variations in Havstensfjorden. Finally, we adjusted the coefficient for Nötesund using the observed salinity variations in Koljöfjorden. The low value of α_{A_o} is probably due to the rather long distance from Åstol to the actual strait, and the fact that the Askerö Straits in turn consist of several sub-basins which are not resolved in the model.

The model generated basin salinities are shown together with observations in Fig. 11. It can not be expected that such a simple model should fully match the observations, particularly since real-time exchange and/or mixing due to tides, local wind, and freshwater, have been neglected. The agreement is close enough, though, to conclude that the model captures the processes which governs the long-term salinity evolution in the system. Apparently, the low sampling frequency allows for events in between the observations. One example is from February–March 1994, when the salinity in Koljöfjorden and Havstensfjorden decreased by about 4 units while the model salinities remained almost constant. The small change in the model can be explained by the rather high 10–20 m salinity at Åstol during this period. The surface water salinity went down, but a decrease of the salinity over the entire external water column is necessary to achieve a strong baroclinic exchange. The most probable cause of the disparity between model results and observations in this case is a decrease of the salinity in-between the monthly BOSAM observations (March 1 and April 5). Another example is in early 1993 when the 10–20 m salinity in Havstensfjorden increased from 25 to 30 without any notable change in the model salinities. This event can be traced to a deepwater inflow, as the salinity at 30–40 m in Havstensfjorden (not shown) also increased from about 32 to 33. A water mass of salinity greater than 33 must have been present outside the fjord for some period, of which there is no sign in the Åstol data. So again, this event must have occurred between the observations.

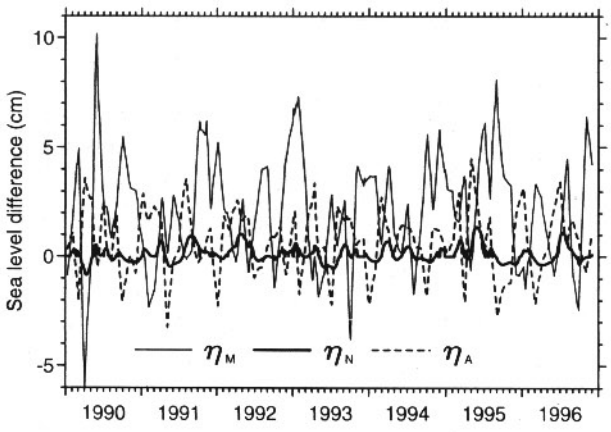

Fig. 12. Computed sea level difference across Malö Strömmar, η_M, across Nötesund, η_N, and across Askerö Straits, η_A. The total difference in steric height, η_S between Åstol and Byttelocket is shown in Fig. 8.

Figure 12 shows the computed sea level differences for each strait separately. The drop across Malö Strömmar is larger than the other two and quite often close to the total difference. The drop across the Askerö Straits reaches a few centimeters at most. The drop over Nötesund is generally modest since the salinity variations are damped in Havstensfjorden, such that the salinity difference is smaller between Havstensfjorden and Koljöfjorden

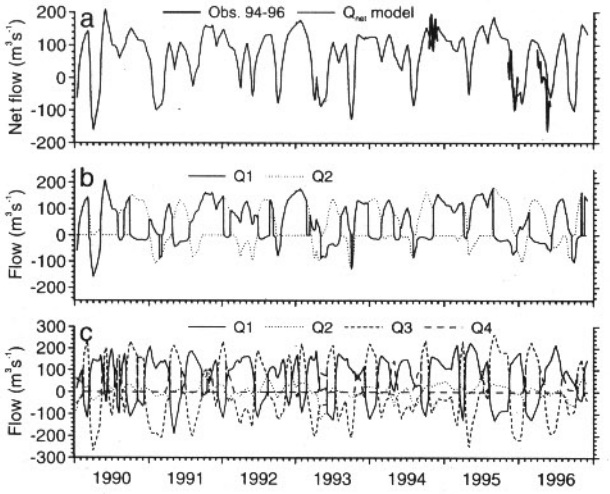

Fig. 13. Modelled and observed flows during 1990 to 1996. (a) Computed net through-flow compared to observed flows (5-d averages) during three shorter periods in 1994, 1995, and 1996 (cf., Fig. 6). The observed flow in Nötesund for 1994 is a weighted average using the width of the strait for each level of ADCP measurements. For 1995 and 1996 the observed velocities in Björnsund were multiplied by the cross section area (325 m^2). (b) Model computed flows in Nötesund, where Q1 is the flow in the upper layer and Q2 the flow in the lower layer. (c) Model computed flows in Askerö Straits. Q1–Q4 refers to the flow in different layers (flow layers) from the surface to bottom. The flow is not entirely defined by this figure since the information about which of the model layers (0–10 m or 10–20 m) that is connected to a certain flow layer is missing. The larger part of the total flow is, however, made up by Q1 and Q3 which are always in the upper and lower model layer, respectively.

than between Åstol and Havstensfjorden. The model computed volume fluxes are shown in Fig. 13. The net flow is generally westward in Nötesund and Malö Strömmar with an amplitude of 100–150 $m^3\ s^{-1}$, interrupted by shorter periods with reversed flow. The flow in Nötesund is often two-layered with opposite directions in the upper and lower layer. The largest flows, sometimes in excess of 200 $m^3\ s^{-1}$, are found in the Askerö Straits, where there is a well-developed baroclinic structure with two or, occasionally, three layers.

Figure 13a compares the calculated net circulation (through-flow) with the observed flows in Nötesund and Malö Strömmar. There is a good agreement during these three short periods, although the model is not capable of resolving the short-term variability that appears in the observations. The model captures the periods of reversed (eastward) flow in Malö Strömmar during 1995 and 1996 and the magnitudes are correct. This result supports the model approach. For the entire 7 yr period we calculated a mean counterclockwise transport of 72 $m^3\ s^{-1}$. This net, subtidal through-flow is in the counterclockwise direction during 81% of the time. The observed, instantaneous velocities in e.g., Nötesund, on the other hand, which are dominated by the tide, are to the west only between 55% and 60% of the time.

The net through-flow is related to a mean sea level difference of 2.8 cm between the southern and northern end of the fjord system. This value fits quite well with an estimated 4.2 cm sea level difference between the tide gauge stations at Varberg and Smögen (Fig. 1) determined geodetically by Ekman (1994). The Varberg–Smögen distance is three times larger than that between Åstol and Byttelocket, but it is likely that a larger part of the total difference is associated with the gradient across the Kattegat-Skagerrak front. The sea level drop is in most cases concentrated to Malö Strömmar, where maximum values may reach 10 cm. The maximum at the other straits is only a few cm. On the other hand, there are several factors which may affect the actual sea level difference apart from the external salinity. When calculating the steric height it is assumed that there is no motion below the 20 m level in the coastal water. The positions of the hydrographic stations could also affect the results, in particular at the northern end where the station is situated some distance from the entrance to the fjord system. The local freshwater supply is small, as mentioned earlier, and should have little effect. The relative importance of freshwater from the river Göta älv, which discharges in the Gothenburg area (Fig. 1), cannot be determined on the basis of presently available data but it may influence the salinity (and the steric height) at the station Åstol (Fig. 2).

Water Exchange

The model indicates that the water exchange in the fjord system is dominated by baroclinic exchange through the southern border since these flows are regularly three to four times larger than the flow through Malö Strömmar (Fig. 13). The net circulation should not be critical for the salinity conditions above sill depth. A test with the model where Malö Strömmar was closed off confirmed this. The root-mean-square difference in salinity between having Malö Strömmar opened or closed is only 0.47 for Koljöfjorden and 0.28/0.22 for the upper/lower layer in Havstensfjorden, respectively.

Although the fjord system as such is dominated by baroclinic exchange imposed from the south, the exchange through Malö Strömmar is not insignificant. Periods with reversed net circulation contribute to a flux of properties from the Skagerrak directly to Koljöfjorden. Occasionally, the deep water in Koljöfjorden may even be renewed by direct inflows through Malö Strömmar, although such events were not seen in our data from 1990–1996. In order to investigate the effect of reversals, a pas-

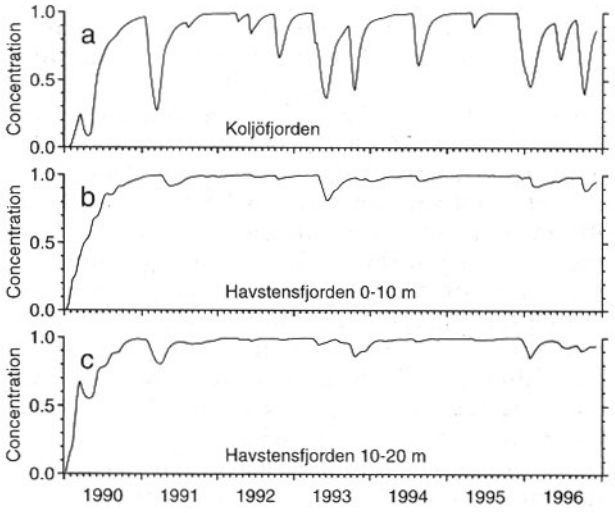

Fig. 14. Modelled concentrations of a tracer in (a) Koljöfjorden, (b) Havstensfjorden 0–10 m, and (c) Havstensfjorden 10–20 m. The tracer concentration is fixed at 1 at Åstol (both boxes) and 0 at Byttelocket.

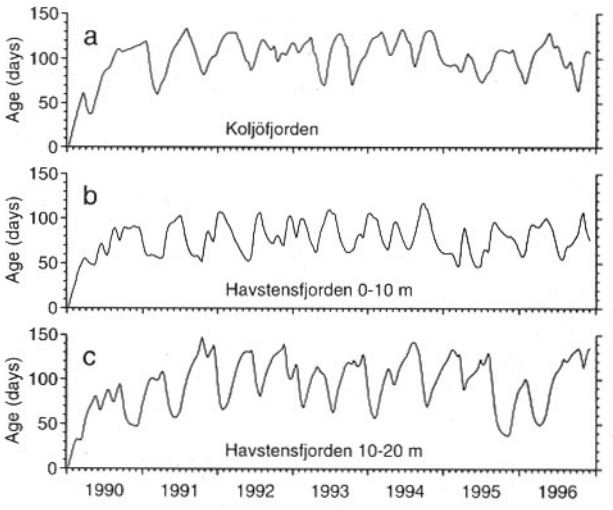

Fig. 15. Modelled age of the water in the different fjord basins, using an age tracer: (a) Koljöfjorden, (b) Havstensfjorden 0–10 m, and (c) Havstensfjorden 10–20 m. The tracer is incremented by the length of the time step for each model time step and is held at concentration 0 at both Åstol and Byttelocket.

sive tracer was introduced into the model. The concentration of this tracer was held at 1 in both boxes at Åstol and 0 at Byttelocket. The tracer concentration inside the fjord system will then reflect the fraction of the water that has penetrated either way. It can be seen from Fig. 14 that the concentration is close to 1 for the entire period in Havstensfjorden, meaning that most of the water there originated at Åstol. In Koljöfjorden, the concentration decreases during events of reversed net circulation (negative values in Fig 13a), such that up to 40% of the water column above sill level sporadically may consist of water having entered through Malö Strömmar. Reversed net circulation is likely to be related to a reversed salinity gradient along the coast which in turn depends on the varying outflow of low-saline Baltic water.

The residence time for a water particle in different parts of the system was estimated by introducing an age tracer. In steady-state, the age is equivalent to the usual definition of the residence time $T = V/Q$, where V is the basin volume and Q the mean water exchange. In our case, the age tracer has value zero in the water entering the fjord system (age 0) and is incremented by the length of the time step at each model time step. The mean residence time is found to be about 80 d in Havstensfjorden and about 100 d in Koljöfjorden (Fig. 15). The age of the water varies in response to the cyclic behavior of the inflows, which is most pronounced in the lower layer in Havstensfjorden where the age varies between 50 and 150 d. These estimates may seem large compared to those presented by Björk (1983) and Axelsson and Rydberg (1993). They give residence times of 6 wk for the surface waters of both fjords. Their estimates, however, are given in relation to the nearest surrounding waters and therefore, the figures are smaller. There is a difference compared to the present estimates, though, which is related to the net circulation, as the former estimates were based on the observations by Ehlin (1971) in Nötesund. His measurements implied a net circulation of 100 $m^3 s^{-1}$ in contrast to the 72 $m^3 s^{-1}$ obtained here, which means that our estimates of the residence times will be higher. It is interesting to note that an age of about 100 d supports the hypothesis of Haamer (1995), who proposed that the algal flora is mainly locally developed.

Conclusions

Using a combination of hydrographic observations and a process-oriented box model, we have shown that the external hydrography dominates the water exchange in most parts of the Orust-Tjörn fjord system. We have also indicated that there is a net circulation of water through the fjord system, which can be related to the difference in steric height between the southern and the northern end. The model shows a net, long-term counterclockwise through-flow averaging about 70 $m^3 s^{-1}$, and baroclinic flows in the Askerö Straits of approximately 200 $m^3 s^{-1}$.

The present model may be improved by incorporating a more detailed physical and topographic description of the system, for example by increasing the vertical resolution, incorporating local

wind mixing and using a larger number of subbasins. Another line of development may be to apply a fully 3-dimensional model. Before commencing any further development one should be aware that the result from any model will to a high degree be dependent on how well the density stratification at the boundaries is known. It is shown here that monthly measurements at the coast provide a useful but not quite acceptable boundary condition. It is obvious from the salinity measurements at Åstol (Fig. 4) that there are large variations in the hydrographic structure on time scales of a few days. These are related to the passages of low pressures and changing winds, and will have a direct influence on the forcing sea level difference and the baroclinic exchange. This points out the need for some sort of regional coastal model that describes the characteristics of low saline outflows from the Kattegat and the position of the Kattegat-Skagerrak front, and provides realistic boundary conditions for a fjord model.

For future model studies, we recommend at least a 1-yr field program consisting of two S-T chains, one at the southern and one at the northern end of the fjord system, as well as observations of the sea level difference across Malö Strömmar. This will give a solid foundation for resolving the circulation and stratification on shorter time scales. For studies of the biogeochemistry of the fjord system, however, the knowledge we now have should be sufficient with few exceptions.

Acknowledgments

The authors are grateful to Dr. Joel Haamer for all his efforts during the field program. Financial support was supplied by the Swedish Environmental Protection Agency. Data was provided by the Swedish Oceanographic Data Centre at the Swedish Meteorological and Hydrological Institute.

Literature Cited

Andersson, L. and L. Rydberg. 1988. Trends in nutrient and oxygen conditions within the Kattegat. *Estuarine, Coastal and Shelf Science* 26:559–79.

Axelsson, R. and L. Rydberg. 1993. Utvärdering av Bohusläns kustvattenkontrollprogram för perioden 1990–92. Hydrografi och näringsämnen (in Swedish). Department of Oceanography, University of Gothenburg, Report no. 19 (Red Series). Gothenburg.

Björk, G. 1983. Vattenutbyte och skiktningsförhållanden i fjordarna innanför Orust och Tjörn (in Swedish). Department of Oceanography, University of Gothenburg, Report no. 5 (Red Series). Gothenburg.

Carlsson, M. 1998. Mean sea level topography in the Baltic sea determined by oceanographic methods. *Marine Geodesy* 21: 203–217.

Ehlin, U. 1971. Oceanografiska förhållanden i fjordsystemet innanför Orust och Tjörn och avloppsutsläppen från de petrokemiska industrierna i Stenungsund. SMHI (Swedish Meteorological and Hydrological Institute), utlåtande till Västerbygdens vattendomstol (in Swedish). Norrköping, Sweden.

Eid, F. M. and M. A. Said. 1995. On the ocean circulation off the Egyptian coast determined from steric height distributions. *Estuarine, Coastal and Shelf Science* 40:231–237.

Ekman, M. 1994. Deviations of the mean sea-level form the mean geoid in the transition area between the North Sea and the Baltic Sea. *Marine Geodesy* 17:161–168.

Engqvist, A. and A. Omstedt. 1992. Water exchange and density structure in a multi-basin estuary. *Continental Shelf Research* 12:1003–1026.

Gillibrand, P., W. Turell, and A. J. Elliot. 1995. Deep-water renewal in the upper basin of Loch Sunart, a Scottish fjord. *Journal of Physical Oceanography* 25:1488–1503.

Gustafsson, B. 1999. High frequency variability of the surface layers in the Skagerrak during SKAGEX. *Continental Shelf Research* 19:1021–1047.

Gustafsson, B. and A. Stigebrandt. 1996. Dynamics of the freshwater-influenced surface layers in the Skagerrak. *Journal of Sea Research* 35:39–53.

Haamer, J. 1995. Presence of the phycotoxin okadaic acid in mussels (*Mytilus edulis*) in relation to nutrient concentrations in a Swedish coastal water. *Journal of Shellfish Research* 14:209–216.

Nilsson, H. C. and R. Rosenberg. 1997. Benthic habitat quality assessment of an oxygen stressed fjord by surface and sediment profile images. *Journal of Marine Systems* 11:249–264.

Liungman, O., L. Rydberg, and G. Björk. 1996. Data report on measurements of currents, sea-levels and hydrography in the Orust-Tjörn fjord system. Report no. C5. Earth Sciences Centre, University of Gothenburg, Gothenburg.

Lizitzin, E. 1974. Sea Level Changes. Elsevier Oceanography Series 8. Amsterdam.

Patullo, J., W. Munk, R. Revelle, and E. Strong. 1955. The seasonal oscillation in sea level. *Journal of Marine Research* 14: 88–156.

Ridgway, K. R. and J. S. Godfrey. 1997. Seasonal cycle of the East Australian Current. *Journal of Geophysical Research* 102: 22921–22936.

Rydberg, L., J. Haamer, and O. Liungman. 1996. Fluxes of water and nutrients within and into the Skagerrak. *Journal of Sea Research* 35:23–38.

Rodhe, J. 1996. On the dynamics of the large-scale circulation of the Skagerrak. *Journal of Sea Research* 35:9–21.

Stigebrandt, A. 1980. Barotropic and baroclinic response of a semi-enclosed basin to barotropic forcing from the sea, p. 141–164. *In* H. J. Freeland, D. M. Farmer, and C. D. Levings (eds.), Fjord Oceanography. Plenum, New York.

Stigebrandt, A. 1984. Analysis of an 89 year long sea level record from the Kattegat with special reference to the barotropically driven water exchange between the Baltic and the sea. *Tellus* 36:401–408.

Stigebrandt, A. 1990. On the response of the horizontal mean vertical density distribution in a fjord to low-frequency density fluctuations in the coastal water. *Tellus* 42:605–614.

Tomczak, M. and S. Godfrey. 1994. Regional Oceanography: An Introduction. Pergamon, Oxford.

Source of Unpublished Material

Cederlof, U. and L. Djurfeldt. Personal Communication. University of Gothenburg, Department of Oceanography, Gothenburg, Sweden.

Received for consideration, June 17, 1999
Accepted for publication, January 31, 2000

Appendix

Consider a very short, frictionless channel with homogeneous water. In the quasi-stationary case we then expect a balance be-

tween the pressure gradient and inertial forces, i.e., the equation of motion reduces to

$$\vec{v} \cdot \nabla \vec{v} = -\frac{1}{\rho} \nabla p \tag{A1}$$

$\vec{v}$ is the velocity vector and p the pressure field. Integrating from far upstream, where $|\vec{v}| \ll |u|$, to the channel, where $|\vec{v}| = |u|$, we get the Bernoulli equation

$$\eta_1 = \frac{u^2}{2g} \tag{A2}$$

where η_1 is the sea level drop necessary to accelerate the water into the channel. If we now include friction and consider a channel of length L and constant cross-sectional area A, then a balance between frictional and pressure gradient forces yields

$$\rho \eta_2 g A = \rho C_D u^2 B L \tag{A3}$$

where we have assumed a quadratic bottom stress. η_2 is the sea level drop due to friction, B is the length of the wet perimeter. The total sea level difference along the channel is then given by the sum of the Bernoulli and the friction effects (e.g., Stigebrandt 1980). Eqs. A2 and A3 then yield

$$|h_1 - h_2| = \left(1 + 2C_D \frac{BL}{A}\right) \frac{u^2}{2g} \tag{A4}$$

where h_1 and h_2 are the sea levels at each end of the channel. The expression within brackets is termed C_m in Eq. 1. In the specific case of Malö Strömmar, there is not one channel but two, connected by a small sub-basin (Fig. 2). Assuming that friction is negligible in the sub-basin, the following two quasi-stationary equations may be formed:

$$|h_1 - h| = C_1 \frac{u_1^2}{2g} \tag{A5}$$

$$|h - h_2| = C_2 \frac{u_2^2}{2g} \tag{A6}$$

where the subscripts 1 and 2 indicate which of the two channels to consider and h is the sea level in the sub-basin. Conservation of volume in the sub-basin yields

$$\frac{dh}{dt} = \frac{(u_1 A_1 - u_2 A_2)}{S} \tag{A7}$$

Here, S is the surface area of the sub-basin. Combining Eqs. A5–A7 we find an expression for the time derivative of h in terms of $h_{1(2)}$, $C_{1(2)}$, $A_{1(2)}$, and S. Knowing the geometrical quantities for the two channels and the sub-basin, we can solve for h for a given set of forcing sea levels $h_{1(2)}$. For simplicity, these were chosen as simple sinusoidal functions with a period of 12.4 h (the dominating M2 tidal component), mean values $\eta/2$ and $-\eta/2$, and a phase difference of 70 min (Liungman et al. 1996). Having determined h, we can then calculate the transport and its mean using either Eq. A5 or A6. The resulting tidal choking (i.e., the reduction in the mean transport with increasing tidal amplitude, for a given mean sea level difference of η) is a result of the existence of the sub-basin and the limited transport capacity of the interconnecting channel.